Bioorg. Med. Chem. Lett. 87 (2023) 129260

Contents lists available at ScienceDirect

Bioorganic & Medicinal Chemistry Letters

journal homepage: www.elsevier.com/locate/bmcl

Maleimide constrained BAD BH3 domain peptides as BCL-x_L Inhibitors: A versatile approach to rapidly identify sites compatible with peptide constraining

Peiyu Zhang [a,b], Martin Walko [a,b], Andrew J Wilson [a,b,*]

[a] School of Chemistry, University of Leeds, Woodhouse Lane, Leeds, LS2 9JT, UK
[b] Astbury Centre for Structural Molecular Biology, University of Leeds, Woodhouse Lane, Leeds LS2 9JT, UK

ARTICLE INFO

Keywords:
Protein-protein interactions
Constrained peptides
BAD
BCL-x_L

ABSTRACT

Development of protein–protein interaction (PPI) inhibitors remains a major challenge. A significant number of PPIs are mediated by helical recognition epitopes; although peptides derived from such epitopes are attractive templates for inhibitor design, they may not readily adopt a bioactive conformation, are susceptible to proteolysis and rarely elicit optimal cell uptake properties. Constraining peptides has therefore emerged as a useful method to mitigate against these liabilities in the development of PPI inhibitors. Building on our recently reported method for constraining peptides by reaction of dibromomaleimide derivatives with two cysteines positioned in an i and $i + 4$ relationship, in this study, we showcase the power of the method for rapid identification of ideal constraining positions using a maleimide-staple scan based on a 19-mer sequence derived from the BAD BH3 domain. We found that the maleimide constraint had little or a detrimental impact on helicity and potency in most sequences, but successfully identified i, $i + 4$ positions where the maleimide constraint was tolerated. Analyses using modelling and molecular dynamics (MD) simulations revealed that the inactive constrained peptides likely lose interactions with the protein as a result of introducing the constraint.

Inhibition of protein–protein interactions (PPIs) using synthetic reagents has historically been considered challenging given the interfaces between two proteins are usually large, lack well-defined recognition pockets and can position recognition handles in a spatially disconnected manner with respect to one another.[1,2] In comparison to small molecules, peptides have larger sizes and can effectively mimic native binding motifs of proteins. Thus peptides serve as promising templates for development of synthetic PPI inhibitors.[3–7] However, peptides composed of natural amino acids may not readily adopt a bioactive conformation and suffer from poor proteolytic stability, poor cell permeability and rapid clearance.[8–11] Peptide constraining is one of the strategies to overcome these barriers,[8,11–13] and has stimulated intense efforts to target helix mediated PPIs since a hydrocarbon "stapled" peptide based on the BID BH3 domain was reported by Walensky *et al.*;[14] a significant number of synthetic strategies for constraining peptides in a helical conformation have been disclosed.[15–20] Similarly, peptides based on various BH3 domains of BCL-2 family proteins have served as prominent models for development of new constraints and targets for early stage drug discovery programs.[8,21] We recently reported a method for generating constrained peptides using dibromomaleimide and demonstrated that this method shows promise in generating constrained peptides with enhanced biophysical and proteolytic properties.[22–24] This approach relies on reaction of dibromomalimide derivatives with two cysteines positioned in an i and $i + 4$ relationship; the reaction proceeds rapidly (hrs) in aqueous mixtures on unprotected peptides and exploits commercially available natural amino acids. In the current manuscript we showcase the power of the maleimide constraining approach for rapid identification of optimal positions to introduce a constraint in a helical binding epitope. We chose the BAD/BCL-x_L PPI as a model and performed a maleimide constraint scan following *in silico* identification of potential hot-residues on a peptide derived from the BAD BH3 domain. We identified the tolerated positions for installation of a maleimide constraint using fluorescence anisotropy assays. Further analyses of the secondary structural preferences of the peptides using circular dichroism spectroscopy, together with molecular modelling and molecular dynamics (MD) simulations are consistent with a bind-and-fold mechanism of recognition between BAD and BCL-x_L, and, that loss of inhibitory potency can arise due to interference with the

* Corresponding author.
E-mail address: a.j.wilson@leeds.ac.uk (A.J. Wilson).

https://doi.org/10.1016/j.bmcl.2023.129260
Received 14 November 2022; Received in revised form 23 March 2023; Accepted 24 March 2023
Available online 28 March 2023

ability to present hot-spot residue side chains in an ideal orientation for BCL-x_L recognition, by the constraint.

The BCL-2 family proteins regulate the intrinsic cell death pathway through PPIs to control mitochondrial outer membrane permeabilization (MOMP).[25–26] Several family members promote programmed cell death (apoptosis), e.g. the effectors BIM, BID, BAD, PUMA and the multidomain pore forming BAK and BAX; whilst other anti-apoptotic (pro-survival) members, e.g. BCL-2, BCL-x_L, MCL-1 and BFL-1, block apoptosis through association with the pro-apoptotic members.[25–26] The BCL-2 family have therefore served as powerful models to elaborate new methods to target PPIs[15,27,28] and represent important therapeutic targets,[26,29,30] Bcl-2 agonist of cell death (BAD) is one of the BH3-only members (which only have BH3 domains) of the BCL-2 family; it plays important roles in diverse biological processes, e.g. apoptosis and glucose metabolism.[31–33] The BAD BH3 domain associates with anti-apoptotic proteins, e.g. BCL-x_L, BCL-2 and BCL-W, to trigger apoptosis by releasing the multidomain proteins BAX and BAK to form a pore in the mitochondrial membrane. Phosphorylation modulates the apoptotic function of BAD;[34] when dephosphorylated, BAD can bind to anti-apoptotic members e.g. BCL-2, BCL-x_L, and BCL-W.[35,36] However, upon phosphorylation BAD interacts with the adaptor protein 14-3-3 and its apoptotic function is suppressed.[37] Moreover, prior studies showed that in the phosphorylated state, BAD causes glucokinase activation and is thus relevant to glucose metabolism.[35,38] Therefore, mimicry of the PPI between an anti-apoptotic protein and BAD can theoretically promote apoptosis and may serve as a viable approach for treatment of cancer. Previous studies identified constrained peptides based on the BAD BH3 domain.[39,40] Danial and co-workers demonstrated that hydrocarbon stapled phospho-BAD BH3 mimetics can activate glucokinase via an allosteric mechanism.[40] Fairlie and co-workers developed truncated BAD BH3 peptides containing one or more lactam bridges. A number of peptides with multiple constraints showed improved *in vitro* binding efficiency indices in a fluorescence polarization assay and cytotoxicity in an MTT assay.[41]

Alanine scanning is commonly used to identify hot-spot residues at a protein–protein interface, i.e. those that contribute significantly (>4.2 kJ/mol) to the binding free energy.[42,43] Appropriately implemented computational approaches to alanine scanning can be quicker and lower-cost in comparison to experimental approaches.[44] Therefore, we first performed a virtual alanine scan using the BUDE[45] Alanine Scan (BAlaS) web interface[46] to identify potential hot-spot resides in the BAD BH3 sequence. To perform these analyses we used the human BAD/BCL-x_L structure (PDB ID: 1G5J)[47] and for comparison, a further crystal structure of the complex between BAD and an anti-apoptotic analogue of BCL-x_L from zebra fish (BAD/NRZ, PDB ID:6FBX).[48] Several residues were predicted to be potential hot-spot residues in the BAD/BCL-x_L interaction, including Leu104, Tyr110, Leu114, Arg115, Phe121 and Phe125 (Fig. 1a). Significantly, Phe121 and Phe125 exhibited a significant calculated increase in binding free energy when replaced with alanine (18 kJ/mol and 13.2 kJ/mol respectively), highlighting important roles of these two residues for recognition of BCL-x_L. The alanine scan of the BAD peptide in complex with NRZ predicted Tyr95, Leu99, Arg100 and Phe106 as residues with a significant contribution to the binding free energy associated with BCL-x_L recognition (Fig. 1b). The prediction of residues is consistent with the typical h1, h2, h3, hydrophobic residue constellations observed in BCL2 family interactions,[49–50] and together with the similarity of the virtual alanine scanning results using the BAD BH3 domain and different multidomain BCL-2 family proteins provided additional confidence in informing the design of constrained BAD peptidomimetic analogues.

Inspection of the BAD/BCL-x_L NMR ensemble structure confirmed that the four hydrophobic hot-spot residues, Tyr110, Leu114, Phe121 and Phe125, are grafted on the same surface of the α-helix and insert into the hydrophobic cleft of the BCL-x_L (Fig. 1c). The aromatic residues, Phe121 and Phe125 of BAD, interact with Phe97 and Tyr195 of BCL-x_L *via* π-π interactions, respectively. Notably, the conserved Asp119 forms a charge reinforced hydrogen-bond with Arg139 of BCL-x_L. Similarly, in the interaction between BAD and NRZ, Tyr95, Leu99, Phe106 are located on the same surface of the α-helix and insert into the hydrophobic cleft of NRZ; Asp104 forms a charge-reinforced hydrogen bond with Arg90 of NRZ (not shown in Fig. 1d); the role of Gln110 as a hot-residue is less clear, however Arg100 is engaged in charge reinforced hydrogen-bonding interaction with Glu79 and Asp83 simultaneously. Notably, the two lysine residues, Lys93 and Lys94 were also predicted to be hot- residues. The crystal structure indicates that the side chains of each lysine residue orient in opposing directions to interact with Glu79

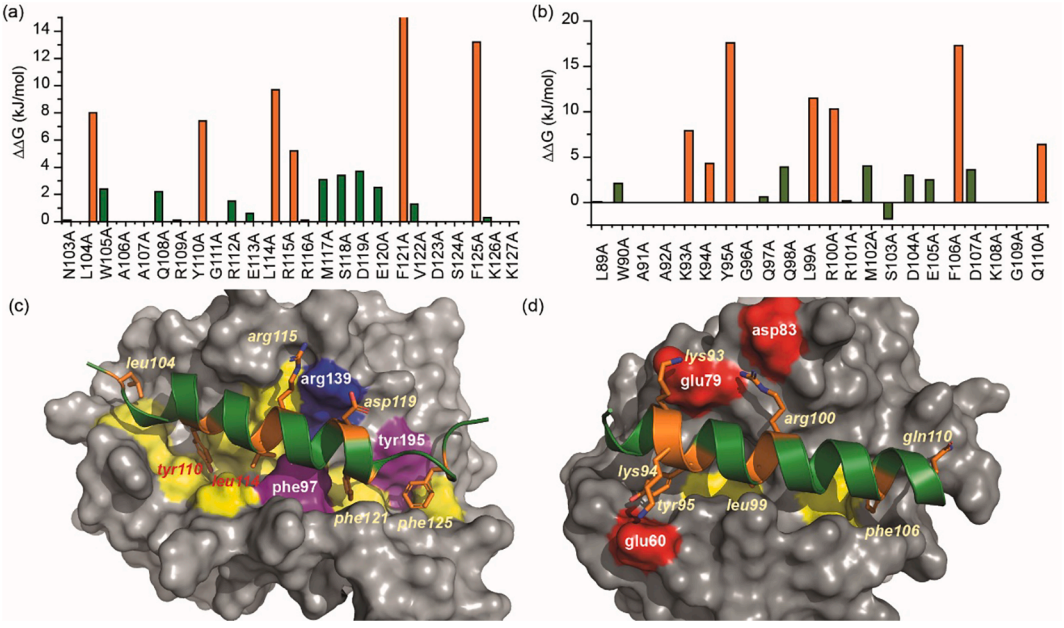

Fig. 1. Virtual alanine scanning results using BALaS and structural analyses for interaction of BAD with BCL-2 family partners: (a) results for BAD/BCL-x_L (PDB ID: 1G5J); (b) results for BAD/NRZ (PDB ID: 6FBX); (c) key interactions for BAD/BCL-x_L (PDB ID: 1G5J); (d) key interactions for zebrafish BAD/NRZ (PDB ID:6FBX) (hot-residues and the conserved asp119 in the BAD peptides are coloured orange; BCL-x_L residues involved in recognition of BAD or NRZ are coloured: yellow for hydrophobic, blue for hydrogen-bonded, purple for π-π interaction and red for charge reinforced hydrogen-bond).

and Glu60 in NRZ (Fig. 1d).

To determine the affinity of BAD-based peptides, we established a direct fluorescence anisotropy assay. Due to the high affinity of long BAD-based peptides, a 19-mer BAD fluorescent tracer was used in this study (FAM-Ahx-$BAD_{109–127}$).[51] In our direct titration assay, FAM-Ahx-$BAD_{109–127}$ was found to bind to BCL-x_L with an affinity $K_d = 119 \pm 23$ nM (Fig. 2a). We also used MCL-1 to investigate the selectivity of the BAD sequence; as anticipated based on literature precedent, FAM-Ahx-$BAD_{109–127}$ failed to exhibit any change in anisotropy up to a concentration of 100 μM MCL-1 (Fig. 2b), suggesting that the 19-mer sequence has excellent selectivity and serves as a good starting point for designing BAD-based peptidomimetic BCL-x_L inhibitors.

Next we applied our recently reported fast and efficient peptide constraining method using dibromomaleimide at i and $i + 4$ positions[22–24] to design, synthesis and biophysical evaluation of a series of BAD-BH3 variant peptides. To do this, pairs of i and $i + 4$ residues in the wild-type $BAD_{109–127}$-BH3 sequence were replaced by cysteines for constraining. To retain the hot-spot residues at the binding interface and minimise the influence arising from replacement of native residues, cysteines were incorporated to avoid changing the relatively hydrophobic hot-spot residues Leu104, Tyr110, Leu114, Phe121 and Phe125, identified from the virtual alanine scan.

This led to 8 bis-cysteine variants (BADL1-L8) based on $BAD_{109–127}$, by incorporating a pair of cysteines at i and $i + 4$ positions from the N-terminus to the C-terminus. Thereafter, we installed a maleimide constraint on each peptide using dibromomaleimide as previously described (see ESI for details of syntheses and peptide characterization),[22–24] and all resultant peptides were tested in fluorescence anisotropy competition assays (Fig. 2c, Table 1 and Fig S1-3). The longer wild-type peptide, $BAD_{103–127}$, gave an $IC_{50} = 0.2 \pm 0.01$ μM, which was more potent than that of the shorter template peptide, $BAD_{109–127}$ (3.6 ± 0.2 μM). Several cysteine variants showed comparable IC_{50}'s in comparison to $BAD_{109–127}$. However, BADL2, BADL4 and BADL7 were observed to have diminished inhibitory potency after incorporation of the cysteines, indicating those positions to be unsuitable for amino acid replacement. The loss of inhibitory potency may be attributed to the replacement of Arg115 which interacts with BCL-x_L or Asp119 which is highly conserved across BH3-only ligands and can interact with Arg143 in BCL-x_L.[49–50] Loss of inhibitory potency was observed for most maleimide constrained peptides in contrast to their unconstrained precursors and in comparison to the wild-type sequence. Two constrained peptides, BADS1 and BADS5, showed similar IC_{50}'s to that of the $BAD_{109–127}$ parent. In competition against the BID/MCL-1 interaction these peptides showed poor inhibitory activity (Fig. 2d) indicating the selectivity preference of the parent wild-type sequence to be retained.

Next, we assessed the conformational preference of the peptides. The two wild-type peptides, $BAD_{103–127}$ and $BAD_{109–127}$ were observed to adopt a combination of random coil and helical conformation as assessed by circular dichroism (CD) spectroscopy; helicities of 14% and 10% were determined, respectively (Table 1 and Fig. S4–S6), in agreement with a prior report.[41] In most sequences, the installation of the maleimide linker did not have a significant impact on the observed helicity in comparison to $BAD_{109–127}$ or the corresponding cysteine precursors. One constrained peptide, BADS4, showed improved helicity in comparison to the linear precursor. However, BADS4 did not retain inhibitory potency in the BAD/BCL-x_L fluorescence anisotropy competition experiment. Taken together, these results indicate that: (a) incorporation of a constraint could not restore the loss of potency caused by replacement of native amino acids with cysteines; (b) in-solution α-helicity of the BAD peptides in the absence of the protein has a minimal impact on inhibitory potency and potentially that BAD interacts with BCL-x_L through a bind-and-fold mechanism as has been observed for other BCL-2 family interactions.[53–57].

To further investigate the impact of the maleimide constraint on the structure of the peptides in isolation and their complexes with BCL-x_L, we performed molecular simulations (MD) using YASARA.[58] First, we modelled structures of complexes between each peptide and BCL-x_L and performed energy minimisation. The minimised structures showed that installation of a maleimide constraint does not cause steric clashes in most complexes with the protein (Figs. S7–S15). However, clashes in BADS2/BCL-x_L and BADS6/BCL-x_L were observed, suggesting these positions are not suitable for introducing a maleimide constraint. Thereafter, $BAD_{109–127}$/BCL-x_L, BADL5/BCL-x_L, BADS5/BCL-x_L, BADL8/BCL-x_L and BADS8/BCL-x_L and the unbound peptide ligands were subjected to in-solution MD simulations for 160 ns (Fig. 3 and Figs. S16–S22). The replicate simulations indicate that $BAD_{109–127}$, BADL5 and BADS5 maintain high helicity in the corresponding complexes with BCL-x_L after 160 ns. To calculate helicity of each peptide in the unbound and bound states, the conformer at 50 ns was chosen as a

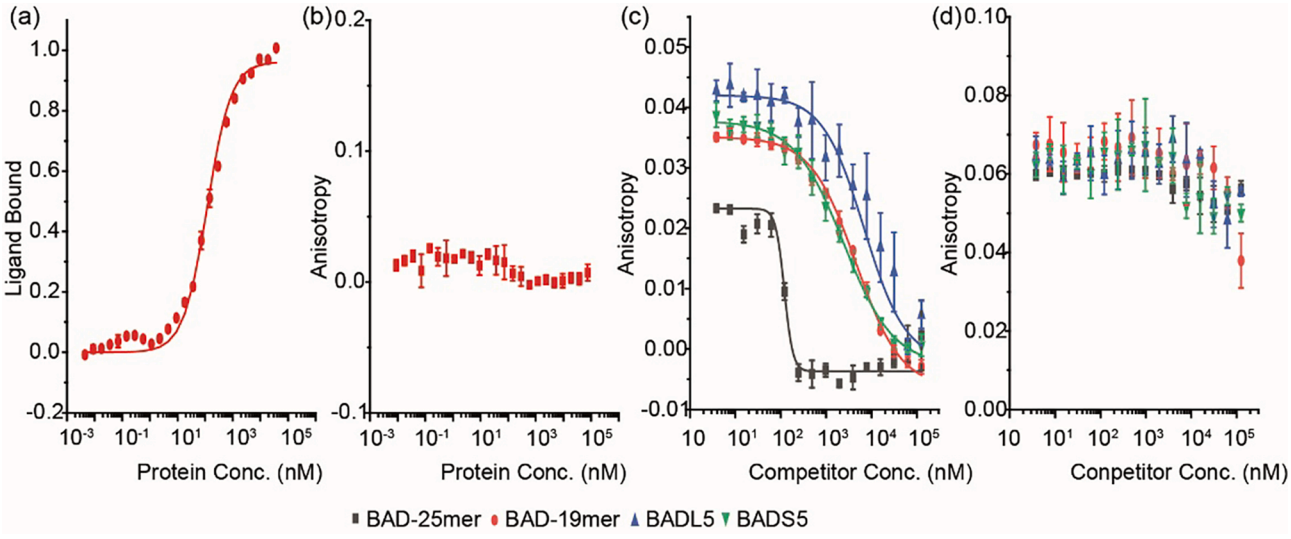

Fig. 2. Fluorescence anisotropy experiments (a) for direct titration of FAM-Ahx-$BAD_{109–127}$ with BCL-x_L (6 nM-125 μM); (b) for direct titration of FAM-Ahx-$BAD_{109–127}$ with MCL-1 (5 nM-105 μM); (FAM-Ahx-$BAD_{109–127}$ = 50 nM, 20 mM Tris, 150 mM NaCl, pH 7.6, 20 °C); (c) Competition FA results for $BAD_{103–127}$, $BAD_{109–127}$, BADL5 and BADS5 against BAD/BCL-x_L (20 mM Tris, 150 mM NaCl, pH 7.6, 200 nM BCL-x_L, 50 nM FAM-Ahx-$BAD_{109–127}$, 20 °C); (b) Competition FA results for $BAD_{103–127}$, $BAD_{109–127}$, BADL5 and BADS5 against BID/MCL-1 (20 mM Tris, 150 mM NaCl, pH 7.6, 150 nM MCL-1, 25 nM FAM-Ahx-BID, 20 °C, note: FAM-Ahx-BID/MCL-1 $K_d \sim 92 \pm 5$ nM).[52]

Table 1
A summary of helicities and FA competition results of the peptides against BCL-x_L.

Peptide	Sequence[a]	IC_{50} BAD/BCL-x_L (μM)[b] (Helicities)[c]	
		Unconstrained(L) 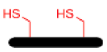	Constrained(S) 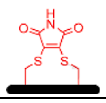
$BAD_{103-127}$	Ac-NLWAAQRYGRELRRMSDEFVDSFKK-NH_2	0.2 ± 0.01 (14%)	
$BAD_{109-127}$	Ac-RYGRELRRMSDEFVDSFKK-NH_2	3.6 ± 0.2 (10 %)	
BADL1/S1	Ac-CYGRCLRRMSDEFVDSFKK-NH_2	5.1 ± 0.7 (11%)	5.5 ± 0.9 (11%)
BADL2/S2	Ac-RYCRELCRMSDEFVDSFKK-NH_2	11.8 ± 1.9(11%)	>50 (10%)
BADL3/S3	Ac-RYGCELRCMSDEFVDSFKK-NH_2	6.8 ± 0.7 (10%)	> 50 (8%)
BADL4/S4	Ac-RYGRELCRMSCEFVDSFKK-NH_2	>50 (8%)	>50 (14%)
BADL5/S5	Ac-RYGRELRCMSDCFVDSFKK-NH_2	6.9 ± 0.4 (9%)	2.4 ± 0.2 (10%)
BADL6/S6	Ac-RYGRELRRMCDEFCDSFKK-NH_2	2.9 ± 0.2 (7%)	> 50 (9%)
BADL7/S7	Ac-RYGRELRRMSCEFVCSFKK-NH_2	> 50 (7%)	> 50 (8%)
BADL8/S8	Ac-RYGRELRRMSDCFVDCFKK-NH_2	4.5 ± 0.4 (10%)	> 50 (10%)

[a] Hot residues are underlined; incorporated cysteines are highlighted in red; a maleimide constraint was added on the cysteines in each BADSn peptide; [b]20 mM Tris, 150 mM NaCl, pH 7.6, 200 nM BCL-x_L, 50 nM FAM-Ahx-$BAD_{109-127}$, 20 °C. [c] [peptide] = 50 μM, 20 mM phosphate, 100 mM NaCl, pH 7.4.

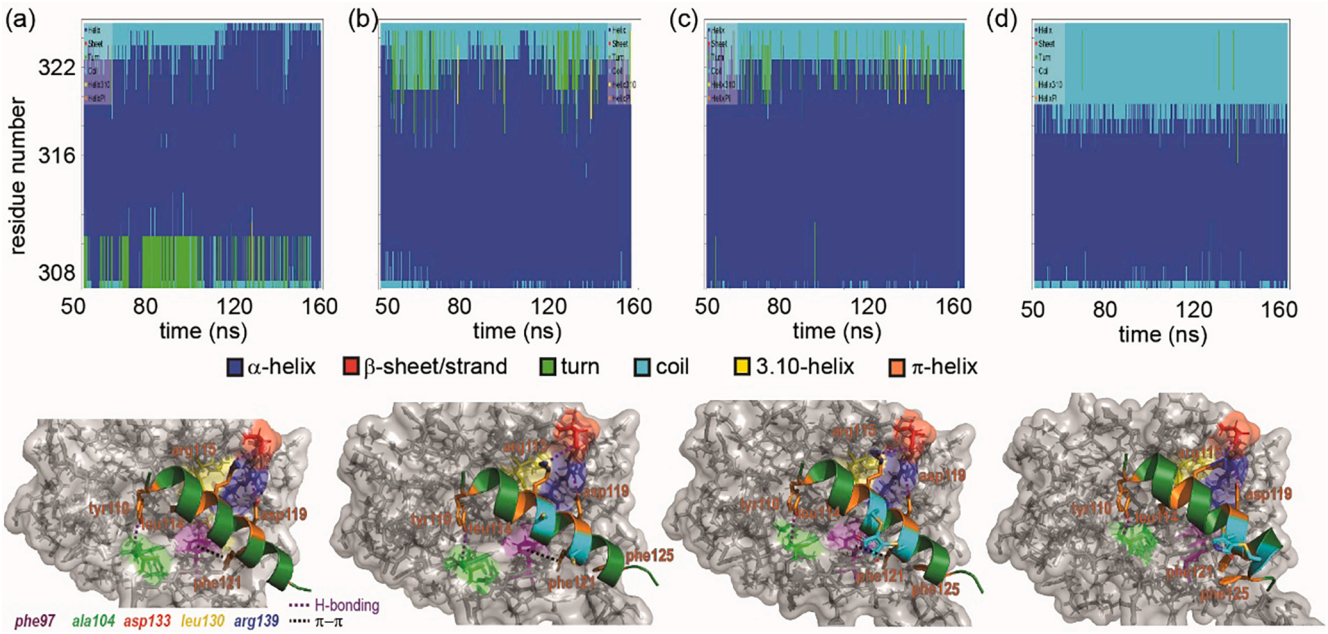

Fig. 3. MD simulation results for different peptide/protein complexes (top = secondary structure content by residue over the timeframe of the simulation, bottom = Interactions in averaged structures from 50 to 160 ns simulation, for replicate simulations see ESI): (a) $BAD_{109-127}$/BCL-x_L; (b) BADL5/BCL-x_L; (c)BADS5/BCL-x_L; (d) BADS8/BCL-x_L.

starting point and helicity from 50 to 160 ns was averaged. In general, the peptides exhibited similar or greater helicity in the bound state than in isolation for both replicate simulations (Table S1). $BAD_{109-127}$ showed an average helicity of 76% in the complex with BCL-x_L (Fig. 3a), whilst BADL5 and BADS5 showed similarly high average helicities of 75% and 82% (Fig. 3b and c), respectively. However, compared with the other three peptides and its linear precursor BADL8 (79% average helicity in bound state), the bound BADS8 gave a lower average helicity (62%) (Fig. 3d), suggesting that introducing a maleimide constraint at this position potentially decreases helicity of the peptide in its bound state leading to a loss of inhibitory potency in agreement with the competition FA results.

We further analysed changes in interactions between the constrained peptides and BCL-x_L in comparison to $BAD_{109-127}$ using the average structures generated by MD simulations; whilst the force fields used limit a quantitative analyses the reproducible observations from replicate simulations can be used to gain an idea as to significant changes in interactions and orientations of side chains. After 160 ns simulation, $BAD_{109-127}$ maintained major interactions observed in the original crystal structure (similar observations are made at different time points). The key interactions between BADL5/BADS5/BADL8 and BCL-x_L were also maintained after the simulations whereas the important Phe121-Phe97 π-π interaction disappeared in BADS8/BCL-x_L average structure (Fig. 3 and Figs. S23–27). These results suggest that the loss of potency may arise from conformational changes resulting in a loss of helicity of bound peptide in combination with a failure to orient key residues optimally for productive interaction between peptide and protein as a consequence of the constraint.

In summary, we have successfully designed maleimide-constrained peptides as BCL-x_L inhibitors with maintained potency and good selectivity based on the BAD BH3 domain. We recently showed the maleimide constraint exhibits comparable or superior impact on helicity and

potency in comparison to other types of staples, e.g. hydrocarbon and xylyl,[59] whilst others have noted that different staples behave differently in different sequence contexts. [60,61] In this work, using a maleimide-staple scan, we identified suitable positions for incorporation of a maleimide constraint in the wild-type peptide. A number of peptides exhibited diminished inhibitory potency as the bis-cysteine and constrained variants, whilst a number exhibited diminished potency only as the constrained variant. Conformational analyses by CD indicated that α-helicity of the peptides in isolation is unlikely to influence inhibitory potency. These unusual results motivated us to use MD simulations to further investigate the bound states of the complexes between peptide ligands and the protein. These MD simulations suggest that differences in bound-state-helicity between the active and inactive constrained peptides likely influence inhibitory potency and that for a number of peptides, constraining modulates the orientation of key side chains such that optimal interaction with BCL-x_L cannot be achieved. These observations highlight the importance of constraint placements in peptide design, and emphasize the complex effects that introducing a constraint can have on potency.[11,23,62]

Author contributions

AJW, PZ and MW conceived and designed the study. PZ performed synthesis and biophysical analyses. PZ and MW performed modelling. PZ and MW performed BCL-x_L expression. The manuscript was written by PZ and edited into its final form by MW and AJW.

Declaration of Competing Interest

The authors declare that they have no known competing financial interests or personal relationships that could have appeared to influence the work reported in this paper.

Data availability

Relevant Data is included in the Supporting Information

Acknowledgements

This work was supported by BBSRC [BB/V008412/1 and BB/V003577/1] and EPSRC [EP/N013573/1]. PZ thanks the University of Leeds and the China Scholarship Council for the financial support. We thank Anastasija Kulik and Amanda Acevedo-Jake for assistance with protein expression. MCL-1 was kindly provided by Amanda Acevedo-Jake. We thank Jeanine Williams for assistance with HPLC purification and analyses.

Appendix A. Supplementary data

Supplementary data to this article can be found online at https://doi.org/10.1016/j.bmcl.2023.129260.

References

1 Yin H, Hamilton AD. Strategies for targeting protein-protein interactions with synthetic agents. *Angew. Chem. Int. Ed.* 2005;44:4130–4163.
2 Scott DE, Bayly AR, Abell C, Skidmore J. Small molecules, big targets: drug discovery faces the protein-protein interaction challenge. *Nat. Rev. Drug Discov.* 2016;15:533–550.
3 Azzarito V, Long K, Murphy NS, Wilson AJ. Inhibition of α -helix-mediated protein-protein interactions using designed molecules. *Nat. Chem.* 2013;5:161–173.
4 Fosgerau K, Hoffmann T. Peptide therapeutics: current status and future directions. *Drug Discov. Today*. 2015;20:122–128.
5 Pelay-Gimeno M, Glas A, Koch O, Grossmann TN. Structure-based design of inhibitors of protein-protein interactions: mimicking peptide binding epitopes. *Angew. Chem. Int. Ed.* 2015;54:8896–8927.
6 Sawyer N, Watkins AM, Arora PS. Protein domain mimics as modulators of protein-protein interactions. *Acc. Chem. Res.* 2017;50:1313–1322.
7 Merritt HI, Sawyer N, Arora PS. Bent into shape: folded peptides to mimic protein structure and modulate protein function. *Pept. Sci.* 2020;112:e24145.
8 Walensky LD, Bird GH. Hydrocarbon-stapled peptides: principles, practice, and progress. *J. Med. Chem.* 2014;57:6275–6288.
9 Jamieson A, Robertson N. Regulation of protein–protein interactions using stapled peptides. *Rep Organ Chem.* 2015;5:65–74.
10 Lau JL, Dunn MK. Therapeutic peptides: historical perspectives, current development trends, and future directions. *Biorg Med Chem.* 2018;26:2700–2707.
11 Wang H, Dawber RS, Zhang P, Walko M, Wilson AJ, Wang X. Peptide-based inhibitors of protein–protein interactions: biophysical, structural and cellular consequences of introducing a constraint. *Chem. Sci.* 2021;12:5977–5993.
12 Zorzi A, Deyle K, Heinis C. Cyclic peptide therapeutics: past, present and future. *Curr. Opin. Chem. Biol.* 2017;38:24–29.
13 Peraro L, Kritzer JA. Emerging methods and design principles for cell-penetrant peptides. *Angew. Chem. Int. Ed.* 2018;57:11868–11881.
14 Walensky LD, Kung AL, Escher I, et al. Activation of apoptosis in vivo by a hydrocarbon-stapled BH3 helix. *Science*. 2004;305:1466–1470.
15 Muppidi A, Doi K, Ramil CP, Wang H-G, Lin Q. Synthesis of cell-permeable stapled BH3 peptide-based Mcl-1 inhibitors containing simple aryl and vinylaryl cross-linkers. *Tetrahedron*. 2014;70:7740-7745.
16 Fairlie DP, Dantas de Araujo A. Review stapling peptides using cysteine crosslinking. *Pept. Sci.* 2016;106:843–852.
17 Peraro L, Zou Z, Makwana KM, et al. Diversity-oriented stapling yields intrinsically cell-penetrant inducers of autophagy. *J. Am. Chem. Soc.* 2017;139:7792–7802.
18 Iegre J, Gaynord JS, Robertson NS, Sore HF, Hyvönen M, Spring DR. Two-component stapling of biologically active and conformationally constrained peptides: past, present, and future. *Adv Therap.* 2018;1:1800052.
19 Li X, Chen S, Zhang W-D, Hu H-G. Stapled helical peptides bearing different anchoring residues. *Chem. Rev.* 2020;120:10079–10144.
20 Dhanjee HH, Saebi A, Buslov I, Loftis AR, Buchwald SL, Pentelute BL. Protein-protein cross-coupling via palladium-protein oxidative addition complexes from cysteine residues. *J. Am. Chem. Soc.* 2020;142:9124–9129.
21 Cromm PM, Spiegel J, Grossmann TN. Hydrocarbon stapled peptides as modulators of biological function. *ACS Chem. Biol.* 2015;10:1362–1375.
22 Grison CM, Burslem GM, Miles JA, et al. Double quick, double click reversible peptide "stapling". *Chem. Sci.* 2017;8:5166–5171.
23 Hetherington K, Hegedus Z, Edwards TA, Sessions R, Nelson A, Wilson AJ. Stapled peptides as HIF-1α/p300 inhibitors: helicity enhancement in the bound state increases inhibitory potency. *Chem Eur J*. 2020;26:7638–7646.
24 Lindsey-Crosthwait A, Rodriguez-Lema D, Walko M, Pask CM, Wilson AJ. Structural optimization of reversible dibromomaleimide peptide stapling. *Pept. Sci.*. 2020:e24157.
25 Kale J, Osterlund EJ, Andrews DW. BCL-2 family proteins: changing partners in the dance towards death. *Cell Death Differ.* 2018;25:65–80.
26 Singh R, Letai A, Sarosiek K. Regulation of apoptosis in health and disease: the balancing act of BCL-2 family proteins. *Nat. Rev. Mol. Cell Biol.* 2019;20:175–193.
27 Yin H, Lee G-I, Sedey KA, et al. Terphenyl-based bak BH3 α-helical proteomimetics as low-molecular weight antagonists of Bcl-xL. *J. Am. Chem. Soc.* 2005;127:10191–10196.
28 Kazi A, Sun J, Doi K, et al. The BH3 α-helical mimic BH3-M6 disrupts Bcl-x_L, Bcl-2, and MCL-1 protein-protein interactions with Bax, Bak, Bad, or Bim and induces apoptosis in a bax- and bim-dependent manner. *J. Biol. Chem.* 2011;286:9382-9392.
29 Ashkenazi A, Fairbrother WJ, Leverson JD, Souers AJ. From basic apoptosis discoveries to advanced selective BCL-2 family inhibitors. *Nat. Rev. Drug Discov.* 2017;16:273–284.
30 Osterlund EJ, Hirmiz N, Pemberton JM, et al. Efficacy and specificity of inhibitors of BCL-2 family protein interactions assessed by affinity measurements in live cells. *Sci. Adv.* 2022;8:eabm7375.
31 Kelekar A, Chang BS, Harlan JE, Fesik SW, Thompson CB. Bad is a BH3 domain-containing protein that forms an inactivating dimer with Bcl-x(L). *Mol. Cell Biol.* 1997;17:7040–7046.
32 Giménez-Cassina A, Martínez-François Juan R, Fisher Jill K, et al. BAD-dependent regulation of fuel metabolism and KATP channel activity confers resistance to epileptic seizures. *Neuron*. 2012;74:719–730.
33 Ziviani E, Scorrano L. In epilepsy BAD is not really bad. *Neuron*. 2012;74:600–602.
34 Bui N-L-C, Pandey V, Zhu T, Ma L, Basappa LPE. Bad phosphorylation as a target of inhibition in oncology. *Cancer Lett.* 2018;415:177–186.
35 Danial NN, Gramm CF, Scorrano L, et al. BAD and glucokinase reside in a mitochondrial complex that integrates glycolysis and apoptosis. *Nature*. 2003;424:952–956.
36 Polzien L, Baljuls A, Rennefahrt UEE, et al. Identification of Novel in Vivo Phosphorylation Sites of the Human Proapoptotic Protein BAD: PORE-FORMING ACTIVITY OF BAD IS REGULATED BY PHOSPHORYLATION *. *J. Biol. Chem.* 2009;284:28004–28020.
37 Masters SC, Yang H, Datta SR, Greenberg ME, Fu H. 14-3-3 inhibits bad-induced cell death through interaction with serine-136. *Mol. Pharmacol.* 2001;60:1325–1331.
38 Board M, Colquhoun A, Newsholme EA. High km glucose-phosphorylating (Glucokinase) activities in a range of tumor cell lines and inhibition of rates of tumor growth by the specific enzyme inhibitor mannoheptulose1. *Cancer Res.* 1995;55:3278–3285.
39 Braun CR, Mintseris J, Gavathiotis E, Bird GH, Gygi SP, Walensky LD. Photoreactive stapled BH3 peptides to dissect the BCL-2 family interactome. *Chem. Biol.* 2010;17:1325–1333.
40 Szlyk B, Braun CR, Ljubicic S, et al. A phospho-BAD BH3 helix activates glucokinase by a mechanism distinct from that of allosteric activators. *Nat. Struct. Mol. Biol.* 2014;21:36–42.

41 Shepherd NE, Harrison RS, Ruiz-Gomez G, Abbenante G, Mason JM, Fairlie DP. Downsizing the BAD BH3 peptide to small constrained α -helices with improved ligand efficiency. *Org. Biomol. Chem.* 2016;14:10939–10945.
42 Clackson T, Wells J. A hot spot of binding energy in a hormone-receptor interface. *Science*. 1995;267:383–386.
43 London N, Raveh B, Schueler-Furman O. Druggable protein–protein interactions – from hot spots to hot segments. *Curr. Opin. Chem. Biol.* 2013;17:952–959.
44 Ibarra AA, Bartlett GJ, Hegedüs Z, et al. Predicting and experimentally validating hot-spot residues at protein-protein interfaces. *ACS Chem. Biol.* 2019;14:2252–2263.
45 McIntosh-Smith S, Price J, Sessions RB, Ibarra AA. High performance in silico virtual drug screening on many-core processors. *Int. J. High Perform. Comput. Appl.* 2015;29:119–134.
46 Wood CW, Ibarra AA, Bartlett GJ, Wilson AJ, Sessions RB, Woolfson DN. BAlaS: fast, interactive and accessible computational alanine-scanning using BudeAlaScan. *Bioinformatics*. 2020;36:2917–2919.
47 Petros AM, Nettesheim DG, Wang Y, et al. Rationale for Bcl-XL/Bad peptide complex formation from structure, mutagenesis, and biophysical studies. *Protein Sci.* 2000;9:2528–2534.
48 Suraweera CD, Caria S, Järvå M, Hinds MG, Kvansakul M. A structural investigation of NRZ mediated apoptosis regulation in zebrafish. *Cell Death Dis.* 2018;9:967.
49 Certo M, Moore VDG, Nishino M, et al. Mitochondria primed by death signals determine cellular addiction to antiapoptotic BCL-2 family members. *Cancer Cell.* 2006;9:351–365.
50 Chen L, Willis SN, Wei A, et al. Differential targeting of prosurvival Bcl-2 proteins by their BH3-only ligands allows complementary apoptotic function. *Mol. Cell.* 2005;17:393–403.
51 Kong W, Zhou M, Li Q, Fan W, Lin H, Wang R. Experimental characterization of the binding affinities between proapoptotic BH3 peptides and antiapoptotic Bcl-2 proteins. *ChemMedChem*. 2018;13:1763–1770.
52 Fletcher JM, Horner KA, Bartlett GJ, Rhys GG, Wilson AJ, Woolfson DN. De novo coiled-coil peptides as scaffolds for disrupting protein–protein interactions. *Chem. Sci.* 2018;9:7656–7665.
53 Lee EF, Czabotar PE, Yang H, et al. Conformational changes in Bcl-2 pro-survival proteins determine their capacity to bind ligands*. *J. Biol. Chem.* 2009;284:30508–30517.
54 Rogers JM, Steward A, Clarke J. Folding and binding of an intrinsically disordered protein: fast, but not 'diffusion-limited'. *J. Am. Chem. Soc.* 2013;135:1415–1422.
55 Rogers JM, Wong CT, Clarke J. Coupled folding and binding of the disordered protein PUMA does not require particular residual structure. *J. Am. Chem. Soc.* 2014;136:5197–5200.
56 Rogers JM, Oleinikovas V, Shammas SL, et al. Interplay between partner and ligand facilitates the folding and binding of an intrinsically disordered protein. *PNAS*. 2014;111:15420–15425.
57 Miles J, Hobor F, Trinh C, et al. Selective affimers recognize the BCL-2 family proteins BCL-xL and MCL-1 through non-canonical structural motifs. *Chembiochem*. 2021;22:232–240.
58 Krieger E, Vriend G. YASARA View—molecular graphics for all devices—from smartphones to workstations. *Bioinformatics*. 2014;30:2981–2982.
59 Zhang P, Walko M, Wilson AJ. Rational design of Harakiri (HRK)-derived constrained peptides as BCL-xL inhibitors. *Chem. Commun.* 2023;59:1697–1700.
60 Hu K, Li W, Yu M, Sun C, Li Z. Investigation of cellular uptakes of the in-tether chiral-center-induced helical pentapeptides. *Bioconjug. Chem.* 2016;27:2824–2827.
61 de Araujo AD, Lim J, Wu K-C, Hoang HN, Nguyen HT, Fairlie DP. Landscaping macrocyclic peptides: stapling hDM2-binding peptides for helicity, protein affinity, proteolytic stability and cell uptake. *RSC Chem Biol.* 2022;3:895–904.
62 Miles JA, Yeo DJ, Rowell P, et al. Hydrocarbon constrained peptides - understanding preorganisation and binding affinity. *Chem. Sci.* 2016;7:3694–3702.